Organo-Cobalt Mediated Living Radical Polymerization of Vinyl Acetate

Chi-How Peng, Jennifer Scricco, Shan Li, Michael Fryd, and Bradford B. Wayland*

Department of Chemistry, University of Pennsylvania, Philadelphia, Pennsylvania 19104-6323

Received November 9, 2007; Revised Manuscript Received January 14, 2008

ABSTRACT: Vinyl acetate polymerization initiated by azo radical sources in the presence of cobalt(II) tetramesitylporphyrin ((TMP)Co^{II}) shows an induction period followed by an organo-cobalt mediated living radical polymerization (LRP). The induction period corresponds to converting (TMP)Co^{II} to an organo-cobalt porphyrin derivative (organo-Co(TMP)). Living character at low vinyl acetate conversion is demonstrated by a linear increase in molecular weight with conversion, relatively low polydispersity homopolymers, and formation of block copolymers with methyl acrylate ((TMP)Co-PVAc-*b*-PMA). Deviations from ideal LRP occur by radical termination and chain transfer events at moderate conversion of vinyl acetate (VAc). Mechanistic studies demonstrate that the VAc radical polymerization is controlled by a degenerative transfer mechanism that utilizes organo-cobalt complexes as the transfer agent. Kinetic studies are utilized in comparing radical polymerization of vinyl acetate and methyl acrylate that are mediated by organo-cobalt complexes.

Introduction

Substantial effort has been directed toward the control of vinyl acetate (VAc) radical polymerization using living radical polymerization (LRP) methods, including atom transfer radical polymerization,[1,2] degenerative transfer through alkyl iodides,[3] dialkyltellurium,[4] trithiocarbonate,[5,6] xanthate,[7–9] and cobalt acetylacetonate transfer agents.[10–12] The focus of interest in poly(vinyl acetate) (PVAc) stems from the facile conversion to polyvinyl alcohol, which is a water-soluble biocompatible polymer material.[13,14]

Organo-cobalt porphyrin complexes ((Por)Co−P) function as dormant species and latent sources of radicals for living radical polymerization of acrylate monomers.[15,16] Previous studies have shown that (Por)Co−P complexes mediate living radical polymerization by both reversible termination (RT) and degenerative transfer (DT) pathways[15,16] (eqs 1 and 2), which is a mechanistic diversity shared with organo-complexes of tellurium[4,17] and titanium[18,19] transfer agents.

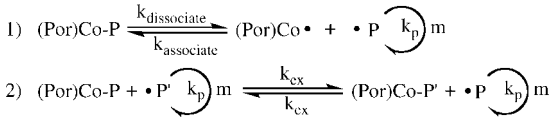

This article reports on an effort to extend the organo-cobalt mediated LRP to vinyl acetate which involves unstabilized high-energy radicals (•CH(OAc)CH$_2$R). The small extent of homolytic dissociation of the relatively strong Co−CH(OAc)CH$_2$R bond makes the RT pathway extremely slow, but interchange of radicals between solution and organo-cobalt complexes of tetramesitylporphyrin (organo-Co(TMP)) provides an effective degenerative transfer route for living radical polymerization of vinyl acetate at 60 °C. Homopolymers and block copolymers are produced at low conversion that have small polydispersity (PDI) and number-average molecular weight (M_n) that approach the theoretical value for one living chain per cobalt porphyrin. Inherent termination and chain transfer events result in substantial deviations from ideal LRP as the conversion increases.

Results and Discussion

Solutions of vinyl acetate (VAc), azo radical sources (azobis(isobutyronitrile) (AIBN), 2,2′-azobis(4-methoxy-2,4-dimethylvaleronitrile) (V-70)), and cobalt(II) tetramesitylporphyrin ((TMP)Co^{II}, Figure 1) when heated at 333 K manifest an induction period prior to the beginning of a first-order radical polymerization process ($\ln([M_0]/[M_t]) = k_p[R^\bullet]t$) (Figure 2).

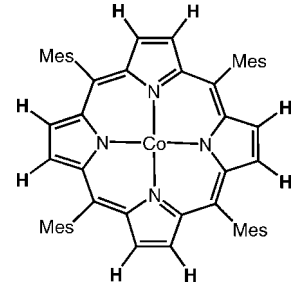

Figure 1. Schematic structure of cobalt(II) tetramesitylporphyrin ((TMP)Co^{II}).

During the induction period radicals that enter solution from the azo radical sources react and are trapped by (TMP)Co^{II} as organo-cobalt complexes. The large difference in the half-lives for unimolecular decay of AIBN ($t_{1/2}$(333 K) = 1110 min) and V-70 ($t_{1/2}$(333 K) = 11 min) makes these radical sources useful for different applications in studying radical polymerization. The slow decay of AIBN gives a near constant radical concentration over time periods of several hours, but V-70 completely decays in a period of only 90 min at 333 K. Mixtures of V-70 and AIBN are used to give a shortened induction period from the rapid decay of V-70 and then an approximately constant influx of radicals from AIBN. If at the end of the induction period radicals continue to enter solution from the azo radical source, then a relatively fast radical polymerization of VAc occurs (333 K) (Figure 2A,B). This is the situation where the control of radical polymerization requires a degenerative transfer mechanism that depends on the exchange of radicals between the solution and the organo-cobalt transfer agent (eq 2). When the number of radicals from the external radical source is insufficient to convert all the (TMP)Co^{II} to organo-cobalt complexes as illustrated in Figure 2C, then this is the condition where the control of radical polymerization uses a reversible termination mechanism (eq 1) where the concentration of radicals in solution is derived exclusively from dissociation of the organo-cobalt complex. The vanishingly small rate of polymerization from radicals that result from Co−R bond homolysis (Figure 2C)

* Corresponding author. E-mail: wayland@sas.upenn.edu.

10.1021/ma702500b CCC: $40.75
Published on Web 02/26/2008

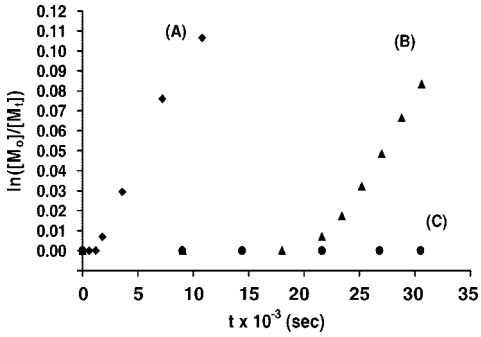

Figure 2. First-order kinetics plots for the radical polymerization of vinyl acetate (VAc) mediated by cobalt(II) tetramesitylporphyrin ((TMP)Co^{II}) in C_6D_6 at 333 K: (A) $[(TMP)Co^{II}]_i = 6.9 \times 10^{-4}$ M, $[V\text{-}70]_i = 8.0 \times 10^{-4}$ M, and $[VAc]_i = 5.42$ M, $R_{(total)}/Co^{II}_i = 1.4$, conversion = 10.11%, PDI (M_w/M_n) = 1.13, M_n = 64 000 ($M_{n(theory)}$ = 68 000). (B) $[(TMP)Co^{II}]_i = 5.9 \times 10^{-4}$ M, $[AIBN]_i = 7.6 \times 10^{-3}$ M, and $[VAc]_i = 1.74$ M, $R_{(total)}/Co^{II}_i = 3.8$, conversion = 8.00%, PDI (M_w/M_n) = 1.22, M_n = 14 000 ($M_{n(theory)}$ = 20 000). (C) $[(TMP)Co^{II}]_i = 5.9 \times 10^{-4}$ M, $[V\text{-}70]_i = 3.9 \times 10^{-4}$ M, and $[VAc]_i = 1.54$ M.

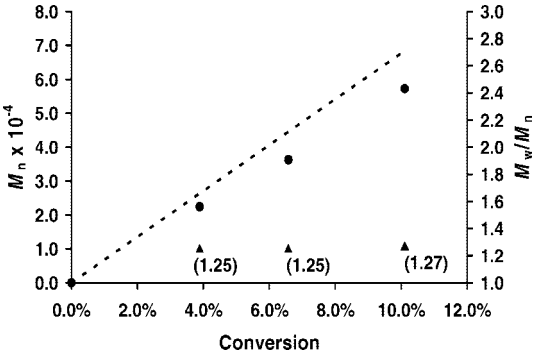

Figure 3. Change in the number-average molecular weight (M_n) (●) and polydispersity (M_w/M_n) (▲) with conversion of vinyl acetate (VAc) to poly(vinyl acetate) (PVAc) at 333 K in C_6D_6. $[VAc]_i = 5.42$ M; $[(TMP)Co^{II}]_i = 6.90 \times 10^{-4}$ M; $[V\text{-}70]_i = 8.00 \times 10^{-4}$ M. The dotted line is the theoretical line for one polymer chain per organo-cobalt complex.

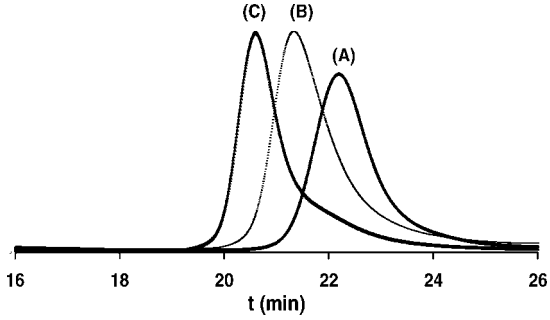

Figure 4. Gel permeation chromatography (GPC) traces illustrating the increase in poly(vinyl acetate) (PVAc) molecular weight (M_n) with vinyl acetate (VAc) conversion in the polymerization system where $[VAc]_i = 5.42$ M; $[(TMP)Co^{II}]_i = 6.90 \times 10^{-4}$ M; and $[V\text{-}70]_i = 8.00 \times 10^{-4}$ M in C_6D_6 at 333 K. (A) M_n = 22 000, PDI (M_w/M_n) = 1.25; (B) M_n = 36 000, PDI (M_w/M_n) = 1.25; (C) M_n = 57 000, PDI (M_w/M_n) = 1.27.

places an upper limit of $\sim 10^{-14}$ on the homolytic dissociation constant (K_{dis}(333 K) $< 10^{-14}$) for organo-cobalt complexes formed by this system.

The polymerization process is observed to have living character during the period of relatively fast radical polymerization after the induction period (Figures 2A,B, 3, and 4). At low vinyl acetate conversion, the number-average molecular weight increases linearly with conversion and relatively small

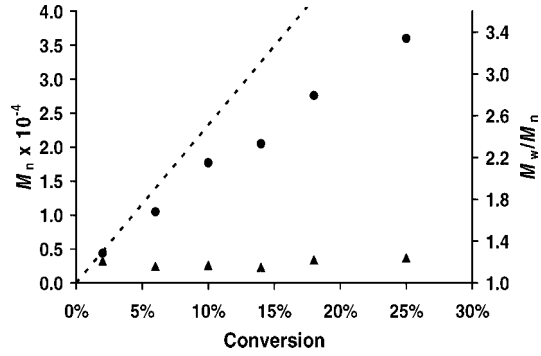

Figure 5. Change in the number-average molecular weight (M_n) (●) and polydispersity (M_w/M_n) (▲) with vinyl acetate (VAc) conversion when $[VAc]_i = 2.7$ M, $[AIBN]_i = 1.7 \times 10^{-3}$ M, $[V\text{-}70]_i = 9.1 \times 10^{-4}$ M, and $[(TMP)Co^{II}]_i = 1.0 \times 10^{-3}$ M in C_6D_6 at 333 K. The dotted line corresponds to the theoretical M_n for one living chain per cobalt porphyrin.

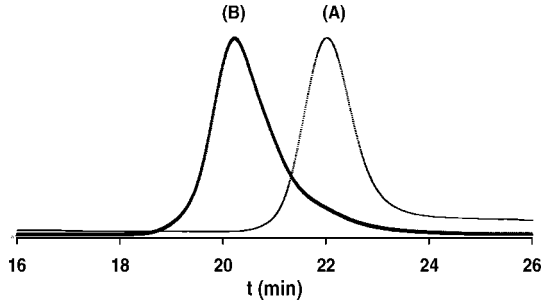

Figure 6. Gel permeation chromatography (GPC) traces in the formation of a poly(methyl acrylate)−poly(vinyl acetate) block copolymer (PMA-*b*-PVAc) mediated by an organo-cobalt complex ((TMP)Co−P). (A) (TMP)Co−PMA block used in forming the PMA-*b*-PVAc block copolymer, M_n = 30 000, PDI (M_w/M_n) = 1.11. (B) Block copolymer of methyl acrylate and vinyl acetate (PMA-*b*-PVAc), M_n = 85 000, PDI (M_w/M_n) = 1.21, conversion = 9.1% in 90 min, $M_{n(PVAc\ block)}$ = 55 000.

polydispersities are observed (Figures 3 and 4). Gel permeation chromatography (GPC) traces used in generating the data presented in Figure 3 are shown in Figure 4. The observed M_n values approach the theoretical values for one living chain per organo-Co(TMP) unit, but deviations toward lower molecular weight regularly increase as the conversion increases (Figures 3−5).

Block copolymers of vinyl acetate with acrylates are readily obtained by sequentially growing the acrylate block on (TMP)Co using AIBN as a radical source, removing the acrylate monomer, and then adding vinyl acetate to grow the PVAc block. One specific example of a diblock copolymer of methyl acrylate (MA) and vinyl acetate (PMA-*b*-PVAc) is shown in Figure 6. The 18.5 h half-life of AIBN at 333 K is much longer than the reaction time of 2 h to form the poly(methyl acrylate) (PMA) block, and thus AIBN remains present in solution to initiate the polymerization of VAc for the second block by a degenerative transfer mechanism. GPC traces for a living poly(methyl acrylate) block attached with (TMP)Co ((TMP)Co−PMA) and the subsequent block copolymer with vinyl acetate ((TMP)Co−PVAc-*b*-PMA) are shown in Figure 6.

The cobalt porphyrin pyrrole ^{1}H NMR for (TMP)Co−PMA is a well-separated AB pattern (Figure 7A(1)), and the pyrrole ^{1}H NMR for the poly(vinyl acetate) complex ((TMP)Co−PVAc) appears as an effective singlet (Figure 7A(2)). The pyrrole hydrogens on adjacent carbon centers of (TMP)Co−PMA and (TMP)Co−PVAc are in theory chemically inequivalent because of the chiral carbon centers of the organo group bonded to cobalt (Co−C*H(X)CH$_2$P). Differences in the anisotropy of the

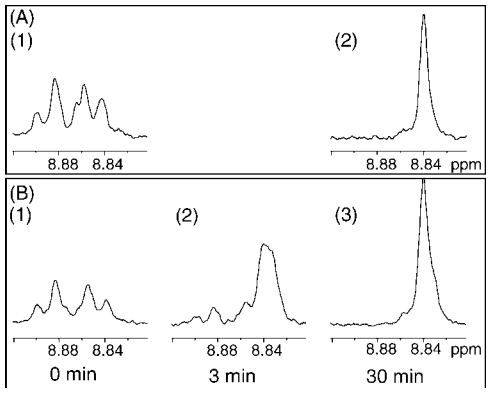

Figure 7. Porphyrin pyrrole ^{1}H NMR (300 MHz; C_6D_6) spectra of polymer organo-cobalt complexes ((TMP)Co−CH(X)CH_2P). The porphyrin pyrrole hydrogens are defined in Figure 1. (A) Homopolymer organo-cobalt porphyrin complexes: (1) (TMP)Co−PMA (poly(methyl acrylate)); (2) (TMP)Co−PVAc (poly(vinyl acetate)). (B) Conversion of (TMP)Co−PMA into a vinyl acetate block copolymer (TMP)Co−PVAc-*b*-PMA at 333 K: (1) t = 0 min, (2) t = 3 min, and (3) t = 30 min.

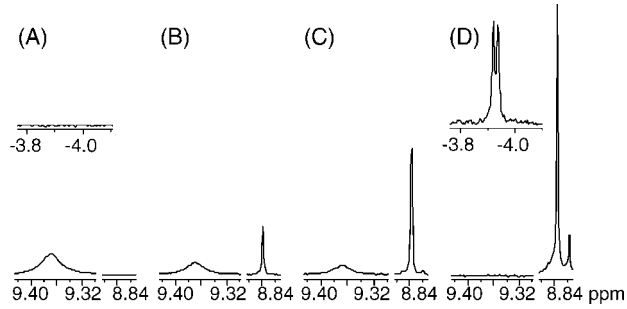

Figure 8. ^{1}H NMR (300 MHz; C_6D_6) spectra illustrating the formation of organo-cobalt complexes (organo-Co(TMP)) during the induction period of vinyl acetate (VAc) polymerization at 333 K. Initial concentrations: $[(TMP)Co^{II}]_i = 1.17 \times 10^{-3}$ M, $[AIBN]_i = 0.0152$ M, $[VAc]_i = 0.13$ M, time = (A) 0 min, (B) 60 min, (C) 120 min, and (D) 300 min.

magnetic susceptibility at the pyrrole hydrogens that arise from the $-CO_2CH_3$ and $-OC(O)CH_3$ (−OAc) groups on the α-carbon are readily observed in the ^{1}H NMR. The ester group from MA produces a substantial chemical shift between adjacent pyrrole hydrogens which appear as an AB pattern in the ^{1}H NMR of (TMP)Co−PMA (Figure 7A(1)), but the acetate group results in virtual chemical equivalence and thus a singlet for the pyrrole ^{1}H NMR of (TMP)Co−PVAc (Figure 7A(2)). Block copolymer formation is readily followed by changes in the organo-cobalt porphyrin pyrrole ^{1}H NMR. Addition of VAc to a solution of (TMP)Co−PMA and AIBN and heating to 333 K results in the decline in intensity for the (TMP)Co−PMA pyrrole ^{1}H NMR AB pattern and appearance of a pyrrole singlet that is characteristic for a vinyl acetate unit bonded with cobalt ((TMP)Co−CH(OAc)CH_2P) (Figure 7B). The time dependence for displacement of the stabilized methyl acrylate type radical unit in (TMP)Co−CH(CO_2CH_3)CH_2PMA by higher energy vinyl acetate type radicals (•CH(OC(O)CH_3)CH_2PVAc) gives a rate constant of 3.8×10^5 at 333 K for exchanging the MA type radical unit by a VAc type radical (k_{ex}(333 K)(PMA•/PVAc•)).

The induction period before onset of VAc radical polymerization results from (TMP)Co^{II} efficiently converting the radicals that enter solution from AIBN or V-70 into an organo-cobalt complex ((TMP)Co−CH(OAc)CH_3). Evolution of the ^{1}H NMR during the induction period is illustrated in Figure 8. Decline in the intensity of the broad *m*-phenyl hydrogen resonance (δ = 9.37 ppm) of the cobalt tetramesitylporphyrin complex reflects the disappearance of the paramagnetic (TMP)Co^{II} and concommitant growth of a narrow singlet (δ = 8.84 ppm) associated with the pyrrole resonance of a diamagnetic organo-cobalt complex (organo-Co(TMP)) (Figure 8).

During the induction period the cyanoisopropyl radicals from AIBN either react with (TMP)$Co^{II•}$ to form (TMP)Co−H (eq 3), which adds with vinyl acetate to form (TMP)Co−CH(OAc)CH_3 (eq 4) or directly react with vinyl acetate to form $(CH_3)_2$(CN)C−CH_2CH(OAc)• (eq 5), which combines with (TMP)$Co^{II•}$ to produce (TMP)Co−CH(OAc)CH_2C(CN)$(CH_3)_2$ (eq 6). Reactions of both (TMP)Co−H and $(CH_3)_2$(CN)C• with vinyl acetate (eqs 4 and 5) probably have higher activation barriers and thus smaller rates than the corresponding reactions of methyl acrylate because of the higher energy associated with radicals derived from vinyl acetate.

$$(CH_3)_2(CN)C^{\bullet} + (TMP)Co^{II\bullet} \rightarrow [(TMP)Co-H] + CH_2{=}C(CH_3)CN \quad (3)$$

$$[(TMP)Co-H] + CH_2{=}CH(OAc) \rightarrow (TMP)Co-CH(OAc)CH_3 \quad (4)$$

$$(CH_3)_2(CN)C^{\bullet} + CH_2{=}CH(OAc) \rightarrow (CH_3)_2(CN)C-CH_2CH(OAc)^{\bullet} \quad (5)$$

$$(CH_3)_2(CN)C-CH_2CH(OAc)^{\bullet} + (TMP)Co^{II\bullet} \rightarrow (TMP)Co-CH(OAc)CH_2C(CN)(CH_3)_2 \quad (6)$$

Assignment of NMR peaks for organo-cobalt porphyrin complexes is aided by the characteristic shifts to high field positions that result from the porphyrin aromatic ring current. The high field doublet resonance (δ = −3.92 ppm, ^3J = 5.3 Hz) shown in the inset of Figure 8D is assigned to a methyl group (−CH(OAc)CH_3) of (TMP)Co−CH(OAc)CH_3. Assignment of the predominant initial organo-cobalt complex to (TMP)Co−CH(OAc)CH_3 is based on identifying each of the organo group ^{1}H NMR resonances (δ_{CH} = 0.48 ppm, quartet, ^3J = 5.3 Hz; δ_{CH_3} = −3.92 ppm, doublet, ^3J = 5.3 Hz; $\delta_{OC(O)CH_3}$ = 0.08 ppm, singlet). Formation of (TMP)Co−CH(OAc)CH_3 occurs by fast hydrogen atom abstraction from a methyl group of the cyanoisopropyl radical ($(CH_3)_2$(CN)C•) by (TMP)Co^{II} followed by addition of the transient cobalt hydride ((TMP)Co−H) to vinyl acetate (eqs 3 and 4).

An induction period is not observed in the absence of (TMP)Co^{II} or when starting with a preformed organometallic complex ((TMP)Co−CH(OAc)CH_3) (Figure 9). The observed rate of vinyl acetate polymerization in the presence of organo-cobalt complexes approaches that of regular radical initiated polymerization, but the absolute rate is slightly reduced. Similar rate reductions are seen for organo-cobalt mediated radical polymerization of acrylates[15,16] and also observed in reversible addition fragmentation chain transfer (RAFT) mediated LRP.[20,21] The reduced rate of polymerization in the presence of (TMP)Co−PVAc corresponds to having a smaller radical concentration ($[R^{\bullet}] = [(k_i/2k_t)[AIBN]]^{1/2}$). The rate of radicals entering solution from AIBN (rate = k_i[AIBN]) is the same in the presence and absence of (TMP)Co−PVAc, and thus the decrease in effective radical concentration must result from an increase in the effective radical termination constant (k_t) when (TMP)Co species are present.[16] The larger effective k_t when (TMP)Co−PVAc is present could result from either the smaller polymer molecular weight which is a feature that is observed for the controlled polymerization (Figure 9) or additional termination mechanisms provided by organo-cobalt complexes.

First-order rate plots at 333 K for radical polymerization of methyl acrylate (MA) and vinyl acetate (VAc) at the same initial molar concentrations of AIBN and (TMP)Co are shown in Figure 10. Vinyl acetate has a longer induction period and

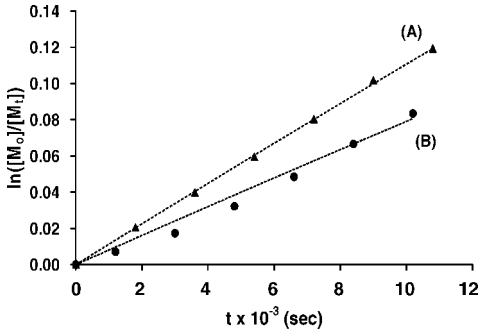

Figure 9. First-order kinetic plots for polymerization of vinyl acetate (VAc) in C_6D_6 at 333 K initiated by AIBN with $[VAc]_i = 1.74$ M and $[AIBN]_i = 7.1 \times 10^{-3}$ M. (A) Absence of (TMP)Co species. Conversion = 11.25%; M_n = 59 000; PDI (M_w/M_n) = 1.58. (B) $[(TMP)Co-CH(Ac)CH_3]_i = 5.86 \times 10^{-4}$ M. Conversion = 8.00%; M_n = 14 000 ($M_{n(theory)}$ = 20 000); PDI (M_w/M_n) = 1.22.

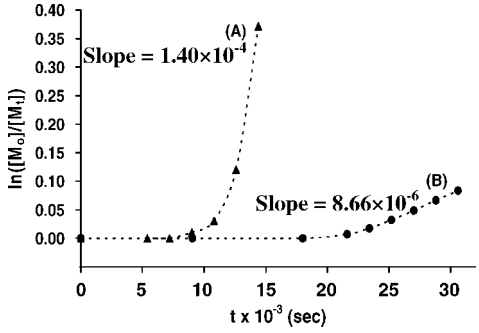

Figure 10. First-order kinetic plots for the radical polymerization in C_6D_6 at 333 K initiated by AIBN ($[AIBN]_i = 7.6 \times 10^{-3}$ M) with (TMP)Co^{II} ($[(TMP)Co^{II}]_i = 5.9 \times 10^{-4}$ M). (A) Methyl acrylate (1.11 M), conversion = 31.03%, PDI (M_w/M_n) = 1.16, M_n = 46 000 ($M_{n(theory)}$ = 50 000). (B) Vinyl acetate (1.74 M), conversion = 8.00%, PDI (M_w/M_n) = 1.22, M_n = 14 000 ($M_{n(theory)}$ = 20 000).

smaller rate of polymerization compared to those of methyl acrylate. The ratio of the slopes of the first-order rate plots shows that the polymerization of MA is 16 times faster than the polymerization of VAc, which results predominately from a larger propagation constant for MA compared to that for VAc. The induction period prior to the onset of polymerization corresponds to the time required to convert (TMP)Co^{II} into organo-Co(TMP) species. The measured induction time for MA corresponds closely to the time required for 1 equiv of radicals to be injected into solution from AIBN per initial equivalent of (TMP)Co^{II}, but the induction time for VAc polymerization corresponds to the time required for ~1.6 equiv of radicals per (TMP)Co^{II} to enter solution (Figure 11). The longer induction period for VAc is tentatively ascribed to inefficient reactions of the stabilized cyanoisopropyl radical ($(CH_3)_2(CN)C^{\bullet}$) to form products of the higher energy unstabilized vinyl acetate radicals ($^{\bullet}CH(OAc)CH_2R$).

GPC traces for PVAc at 10% and 25% VAc conversion produced by the (TMP)Co−P mediated polymerization process using detection by both refractive index and visible electronic spectra (600 nm) are shown in Figure 12. Refractive index detects the entire molecular weight distribution of species, but visible light (600 nm) detection observes only species that have the (TMP)Co chromophore. All of the GPC traces for PVAc produced by organo-cobalt mediated radical polymerization of VAc have a tailing toward low molecular weight that becomes more pronounced as the conversion increases (Figures 4 and 12). The low molecular weight polymers consist of terminated oligomers and lower molecular weight (TMP)Co-capped living

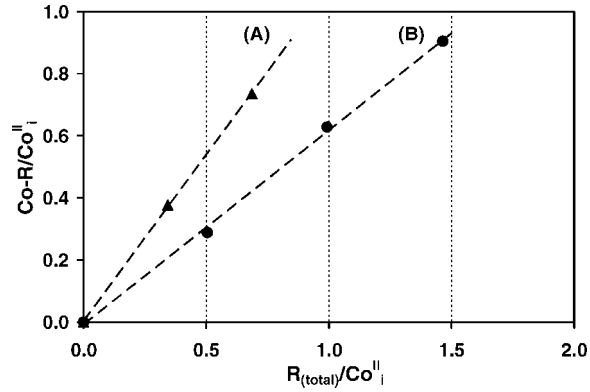

Figure 11. Fraction of (TMP)Co^{II} converted to organo-cobalt complexes (Co−R) as a function of the ratio of equivalents of radical that enter solution from AIBN ($R_{(total)}$) to the initial number of equivalents of (TMP)Co^{II} (Co^{II}_i). (A) Polymerization of methyl acrylate (1.11 M) in C_6D_6 at 333 K initiated by AIBN with $[(TMP)Co^{II}]_i = 5.9 \times 10^{-4}$ M and $[AIBN]_i = 7.6 \times 10^{-3}$ M. (B) Polymerization of vinyl acetate (1.74 M) in C_6D_6 at 333 K initiated by AIBN with $[(TMP)Co^{II}]_i = 5.9 \times 10^{-4}$ M and $[AIBN]_i = 7.6 \times 10^{-3}$ M.

chains that result from reinitiation that uses (TMP)Co^{II} produced in radical termination events.

At 10% conversion the molecular weight distributions observed by refractive index and visible light (600 nm) are nearly superimposable (Figure 12A). When the conversion increases to 25%, a shoulder on a high molecular weight side of the PVAc distribution is observed by 600 nm light detection that is not resolved by refractive index (Figure 12B). This observation is interpreted as evidence for the high molecular weight species containing more than one (TMP)Co complex. Occurrence of PVAc with appended (TMP)Co−PVAc groups and molecular weight approximately twice that of the most probable M_n is most easily explained as occurring through chain transfer by abstraction of a hydrogen from the polymer chain and coupling of the resulting radicals to produce polymers with multiple (TMP)Co chromophore units.

Summary

Vinyl acetate polymerization initiated by azo radical sources (AIBN, V-70) in the presence of cobalt(II) tetramesitylporphyrin ((TMP)Co^{II}) shows an induction period followed by an organo-cobalt-mediated living radical polymerization (LRP). The induction period prior to onset of VAc polymerization corresponds to converting (TMP)Co^{II} to organo-Co(TMP) derivatives. Living character for the radical polymerization at low conversion is indicated by linear increase in molecular weight with conversion, relatively low polydispersity homopolymers, and the capability of forming block copolymers with methyl acrylate ((TMP)Co−PVAc-*b*-PMA). Deviations from ideal LRP occur by radical termination and chain transfer events at moderate conversion. Mechanistic studies demonstrate that the VAc radical polymerization is controlled by an associative degenerative transfer mechanism that utilizes organo-cobalt complexes as the transfer agent.

Experimental Section

Materials. Vinyl acetate (Fluka, 99.0%, 0.0015% hydroquinone inhibitor) and methyl acrylate (Aldrich, 99%, 100 ppm monomethyl ether hydroquinone (MEHQ) inhibitor) were stored in the refrigerator and vacuum-distilled before use. The azo initiators, AIBN ($((CH_3)_2(CN)C)_2N_2$) and V-70 ($((CH_3)_2(OCH_3)C(CH_2)C(CN)-(CH_3))_2N_2$) were purchased from Wako Chemicals USA, Inc., and recrystallized using ethanol for AIBN and methanol for V-70.[23] Cobalt acetate (97%) was supplied by Fisher Scientific and used as received. Tetramesitylporphyrin $(TMP)H_2$ and cobalt(II) tet-

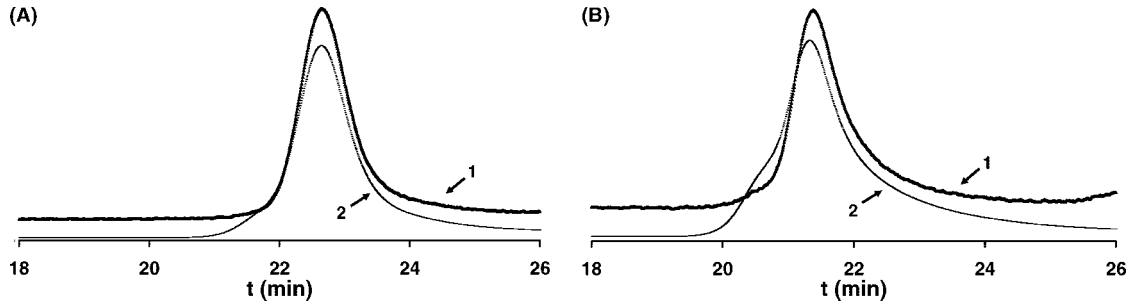

Figure 12. Gel permeation chromatography (GPC) traces of the PVAc product when $[VAc]_i = 2.7M$, $[AIBN]_i = 1.7 \times 10^{-3}$ M, $[V\text{-}70]_i = 9.1 \times 10^{-4}$ M, and $[(TMP)Co^{II}]_i = 1.0 \times 10^{-3}$ M in C_6D_6 at 333 K. Line 1 indicates the refractive index detection trace, and line 2 indicates the visible light (600 nm) detection trace. (A) 10% conversion; (B) 25% conversion.

ramesitylporphyrin ((TMP)Co^{II}) were synthesized following literature methods.[24,25] Solutions of (TMP)Co^{II}, AIBN, V-70, vinyl acetate, and methyl acrylate were subjected to three freeze–pump–thaw cycles to remove any residual oxygen.

Analytical Techniques. Identification of organo-cobalt porphyrin complexes, monomer conversion, and porphyrin structures were evaluated at ambient temperature by ^{1}H NMR spectroscopy using a Bruker AC-360 interfaced to an Aspect 300 computer. Chemical shifts were calibrated relative to deuterated benzene at 7.155 ppm, which was purchased from Cambridge Isotope Laboratory Inc. The percent conversion was determined by intergrating the resonances corresponding to the vinyl protons of the monomer ($\delta_{CH_2CH(OAc)} =$ 4.70 ppm, doublet of doublet, $^3J = 14.0$ Hz, $^2J = 1.4$ Hz; $\delta_{CH_2CH(OAc)} = 4.24$ ppm, doublet of doublet, $^3J = 6.3$ Hz, $^2J = 1.4$ Hz) and the aliphatic protons of the polymer ($\delta_{-CH_2CH(OAc)-} = 5.13$ ppm, broad singlet). The ^{1}H NMR peaks used in measuring the conversion were selected because they have minor overlap with other peaks and thus are more accurate for integrations.

Gel permeation chromatography analysis for polymer products were performed on a Shimadzu modular system, comprised of a Polymer Laboratories 5.0 μm PLgel guard column (50 × 7.5 mm) followed by three linear PLgel columns (10^6, 10^4, and 5×10^2 Å) in an oven (CTO-10A), a UV detector (SPD-10AV) at 600 nm, and a differential refractive index detector (RID-10A), using tetrahydrofuran (THF) as the eluent at 40 °C with a flow rate of 1 mL min^{-1} was used. This system was calibrated using narrow peak width polystyrene standards (Easical, preprepared polymer calibrants purchased from Polymer Laboratories) ranging from 580 to 7.5×10^6 g mol^{-1}.

Polymerization Procedures. Aliquots of the (TMP)Co^{II} and initiator (AIBN or V-70) in C_6D_6 stock solutions were mixed to obtain desired ratios of radical to (TMP)Co^{II} in a vacuum-adapted NMR tube, and a measured volume of the C_6D_6 stock solution of VAc was subsequently injected into the vacuum-adapted tube containing (TMP)Co^{II} and initiator (AIBN or V-70) and subjected to three freeze–pump–thaw cycles to remove dissolved gases. The reaction tube and sample were then placed in a constant temperature bath (60.0 ± 0.1 °C), and the progress of the polymerization was followed by ^{1}H NMR.

One specific polymerization sample was prepared by mixing C_6D_6 solutions of (TMP)Co^{II} (0.40 mL of 7.33×10^{-4} M), AIBN (0.02 mL of 0.19 M), and vinyl acetate (0.08 mL) in a vacuum-adapted NMR tube and subjected to three freeze–pump–thaw cycles. The sample was placed in a 60.0 °C constant temperature bath, and the polymerization was followed by ^{1}H NMR. Monomer conversion reached 8.00% in 510 min, and the number-average molecular weight of the polymeric products was 15 000 with polydispersity of 1.15. The solvent and unreacted monomer were then removed under vacuum, and the dried polymer products were dissolved in THF for the GPC analysis without further purification.

Block Copolymer Synthesis. (TMP)Co^{II} (0.20 mL of 1.38×10^{-3} M), AIBN (0.02 mL of 0.19 M), and methyl acrylate (0.18 mL of 3.70 M) solutions in C_6D_6 were mixed in a vacuum-adapted NMR tube and subjected to three freeze–pump–thaw cycles. The sample was placed in a 60.0 °C constant temperature bath, and the polymerization was followed by ^{1}H NMR. Monomer conversion reached 16.2% in 120 min, and the number-average molecular weight of the polymeric products ((TMP)Co-PMA) was 30 000 with polydispersity of 1.11 (Figure 6A). The solvent and unreacted monomer were then removed under vacuum. Vinyl acetate (0.40 mL of 5.42 M) in C_6D_6 solution was subjected to three freeze–pump–thaw cycles and then added into the vacuum-adapted NMR tube containing (TMP)Co−PMA by vacuum transfer. The sample was placed in a 60.0 °C constant temperature bath again, and the polymerization was followed by ^{1}H NMR. Monomer conversion reached 9.09% in 90 min, and the number-average molecular weight of the block copolymers ((TMP)Co−PVAc-*b*-PMA) was 85 000 with polydispersity of 1.21 (Figure 6B). The solvent and unreacted monomer were then removed under vacuum, and the dried polymer products were dissolved in THF for the GPC analysis without further purification.

Acknowledgment. This research was supported by Grant NSF-CHE-0501198.

References and Notes

(1) Kaneyoshi, H.; Matyjaszewski, K. *J. Polym Sci., Part A: Polym. Chem.* **2007**, *45*, 447–459.
(2) Wakioka, M.; Baek, K.-Y.; Ando, T.; Kamigaito, M.; Sawamoto, M. *Macromolecules* **2002**, *35*, 330–333.
(3) Iovu, M. C.; Matyjaszewski, K. *Macromolecules* **2003**, *36*, 9346–9354.
(4) Kwak, Y.; Goto, A.; Fukuda, T.; Kobayashi, Y.; Yamago, S. *Macromolecules* **2006**, *39*, 4671–4679.
(5) Postma, A.; Davis, T. P.; Li, G.; Moad, G.; O'Shea, M. S. *Macromolecules* **2006**, *39*, 5307–5318.
(6) Ting, S. R. S.; Granville, A. M.; Quémener, D.; Davis, T. P.; Stenzel, M. H.; Barner-Kowollik, C. *Aust. J. Chem.* **2007**, *60*, 405–409.
(7) Destarac, M.; Charmot, D.; Franck, X.; Zard, S. Z. *Macromol. Rapid Commun.* **2000**, *21*, 1035–1039.
(8) Charmot, D.; Corpart, P.; Adam, H.; Zard, S. Z.; Biadatti, T.; Bouhadir, G. *Macromol. Symp.* **2000**, *150*, 23–32.
(9) Theis, A.; Davis, T. P.; Stenzel, M. H.; Barner-Kowollik, C. *Polymer* **2006**, *47*, 999–1010.
(10) Debuigne, A.; Caille, J.-R.; Jèrôme, R. *Angew. Chem., Int. Ed.* **2005**, *44*, 1101–1104.
(11) Debuigne, A.; Willet, N.; Jèrôme, R.; Detrembleur, C. *Macromolecules* **2007**, *40*, 7111–7118.
(12) Maria, S.; Kaneyoshi, H.; Matyjaszewski, K.; Poli, R. *Chem. Eur. J.* **2007**, *13*, 2480–2492.
(13) Lee, K. Y.; Mooney, D. J. *Chem. Rev.* **2001**, *101*, 1869–1880.
(14) Chiellini, E.; Corti, A.; D'Antone, S.; Solaro, R. *Prog. Polym. Sci.* **2003**, *28*, 963–1014.
(15) Wayland, B. B.; Peng, C.-H.; Fu, X.; Lu, Z.; Fryd, M. *Macromolecules* **2006**, *39*, 8219–8222.
(16) Peng, C.-H.; Fryd, M.; Wayland, B. B. *Macromolecules* **2007**, *40*, 6814–6819.
(17) Goto, A.; Kwak, Y.; Fukuda, T.; Yamago, S.; Iida, K.; Nakajima, M.; Yoshida, J. *J. Am. Chem. Soc.* **2003**, *125*, 8720–8721.

(18) Asandei, A. D.; Moran, I. W. *J. Am. Chem. Soc.* **2004**, *126*, 15932–15933.
(19) Asandei, A. D.; Saha, G. *Macromolecules* **2006**, *39*, 8999–9009.
(20) Chiefari, J.; Chong, Y. K.; Ercole, F.; Krstina, J.; Jeffery, J.; Le, T. P. T.; Mayadunne, R. T. A.; Meijs, G. F.; Moad, C. L.; Moad, G.; Rizzardo, E.; Thang, S. H. *Macromolecules* **1998**, *31*, 5559–5562.
(21) Moad, G.; Rizzardo, E.; Thang, S. H. *Aust. J. Chem.* **2005**, *58*, 379–410.
(22) Moad, G.; Rizzardo, E.; Solomon, D. H.; Beckwith, A. L. J. *Polym. Bull.* **1992**, *29*, 647–652.
(23) Fukuda, T.; Ma, Y.-D.; Inagaki, H. *Macromolecules* **1985**, *18*, 17–26.
(24) Lindsey, J. S.; Wagner, R. W. *J. Org. Chem.* **1989**, *54*, 828–836.
(25) Woska, D. C.; Xie, Z. D.; Gridnev, A. A.; Ittel, S. D.; Fryd, M.; Wayland, B. B. *J. Am. Chem. Soc.* **1996**, *118*, 9102–9109.

MA702500B